AM225: Symplectic integration methods

Hamiltonian dynamics is a powerful framework for describing a variety of physical systems where energy is conserved, such as rigid body motion, celestial mechanics, or the motion of charged particles in an electric field. The framework is based upon writing a *Hamiltonian* $H(p,q)$ that usually represents the total energy of the system in terms of a set of generalized coordinate variables $q = (q_1, q_2, \ldots, q_n)$ and generalized momentum variables $p = (p_1, p_2, \ldots, p_n)$. One can derive that the equations of motion of the system are given by

$$\frac{dp_i}{dt} = -\frac{\partial H}{\partial q_i}(p,q), \qquad \frac{dq_i}{dt} = \frac{\partial H}{\partial p_i}(p,q). \tag{1}$$

Hamiltonian systems like Eq. 1 have two remarkable properties:

- The conserve the Hamiltonian. By taking a time derivative of $H(p,q)$ and substituting in the governing equations, one obtains

$$\begin{aligned}\frac{dH}{dt} &= \sum_{i=1}^{n} \dot{p}_i \frac{\partial H}{\partial p_i} + \sum_{i=1}^{n} \dot{q}_i \frac{\partial H}{\partial q_i} \\ &= \sum_{i=1}^{n} \left(-\frac{\partial H}{\partial q_i}(p,q) \right) \frac{\partial H}{\partial p_i} + \sum_{i=1}^{n} \left(\frac{\partial H}{\partial p_i} \right) \frac{\partial H}{\partial q_i} = 0 \end{aligned} \tag{2}$$

  where a dot represents a time derivative. Hence H is a constant.

- The flow is *symplectic*, meaning that it preserves the differential 2-form

$$\omega^2 = \sum_{i=1}^{n} dp_i \wedge dq_i. \tag{3}$$

  Put more simply, the flow in the (p,q) space is volume-preserving.

In general, the ODE integration methods that we have considered so far will not explicitly preserve the above two properties. In this document, we show that it is possible to construct *symplectic integration methods* that do. For certain problems, symplectic methods are a very attractive choice, since it is useful for the numerical method to retain the mathematical structure of the underlying physical system. These notes are based primarily on the textbook by Hairer *et al.* [1] used in the course, and for further details and examples the reader should consult this reference.

Example: an elliptical orbit

Consider the orbit of a small asteroid m around a large star of mass M centered the origin, where $M \gg m$. Let (p_1, p_2) and (q_1, q_2) be the momentum and position of the asteroid in

its plane of motion. The Hamiltonian is

$$H(p,q) = \frac{p_1^2 + p_2^2}{2m} - \frac{GMm}{\sqrt{q_1^2 + q_2^2}} \tag{4}$$

where G is the gravitational constant. By rescaling length and time, the constants GM and m can be eliminated to obtain

$$H(p,q) = \frac{p_1^2 + p_2^2}{2} - \frac{1}{\sqrt{q_1^2 + q_2^2}}. \tag{5}$$

The governing equations are then

$$\frac{dp_1}{dt} = -\frac{q_1}{(q_1^2 + q_2^2)^{3/2}}, \tag{6}$$

$$\frac{dp_2}{dt} = -\frac{q_2}{(q_1^2 + q_2^2)^{3/2}}, \tag{7}$$

$$\frac{dq_1}{dt} = p_1, \tag{8}$$

$$\frac{dq_2}{dt} = p_2. \tag{9}$$

In the early 1600's, Johannes Kepler showed that the solutions to Eqs. 6–9 are ellipses.[1] In polar coordinates (r,θ), the ellipse is given by

$$r(\theta) = \frac{a(1-e^2)}{1 - e\cos\theta}, \tag{10}$$

where a is the semi-major axis and e is the eccentricity. The orbital speed is given by

$$v = \sqrt{\frac{2}{r} - \frac{1}{a}} \tag{11}$$

and the orbital period is

$$T = 2\pi a^{3/2}. \tag{12}$$

For our test problem, we consider the case of $a = 1$ and $e = 1/3$, and start the asteroid at $\theta = 0$. Equations 10 & 11 give initial conditions

$$(p_1, p_2) = (0, 1/\sqrt{2}), \qquad (q_1, q_2) = (4/3, 0). \tag{13}$$

Equation 12 states that the period of this orbit is $T = 2\pi$, and hence we simulate for a duration of 6π corresponding to three complete orbits. A fixed timestep of $\pi/240$ is used. Four different methods are considered:

[1] More generally the solutions could be any conic section, including parabolae and hyperbolae.

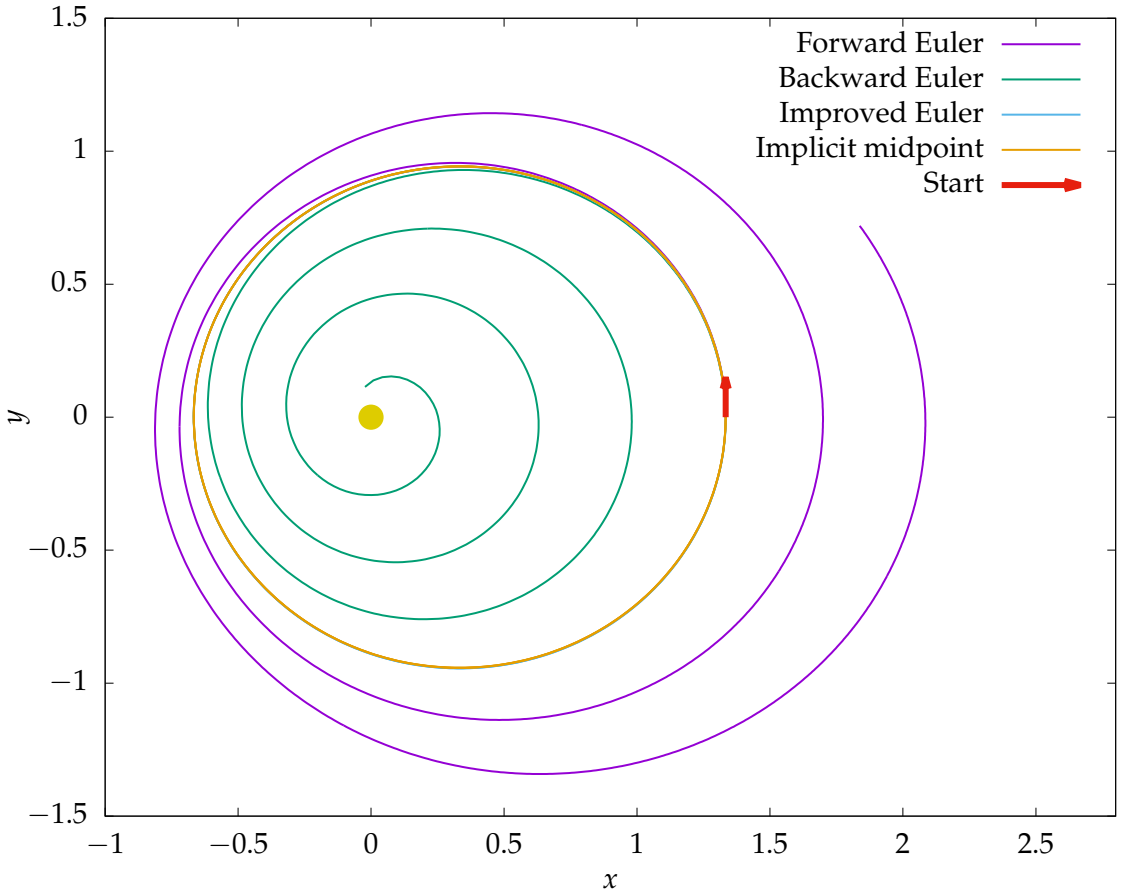

Figure 1: Computed trajectories using four different integration methods for the asteroid orbit test problem. An elliptical orbit with semi-major axis $a = 1$ and eccentricity $e = 1/3$ is used. The vector shows the initial position and direction of the asteroid. The yellow circle indicates the position of the star.

1. The explicit forward Euler method, $y_{n+1} = y_n + hf(y_n)$.
2. The implicit backward Euler method, $y_{n+1} = y_n + hf(y_{n+1})$.
3. The implicit midpoint rule, $y_{n+1} = y_n + hf(\frac{y_n + y_{n+1}}{2})$.
4. The improved Euler method, $k_1 = f(y_n)$, $k_2 = f(y_n + hk_1)$, $y_{n+1} = y_n + \frac{h(k_1+k_2)}{2}$.

Figure 1 shows plots of the asteroid trajectory with the four methods. The forward Euler method gradually spirals outward, thereby gaining energy, while the backward Euler method gradually spirals inward, thereby losing energy. The backward Euler integration terminates prematurely at $t \approx 10.27$ due to the root-finding method not converging. Even though a small timestep is used, both of these methods quickly lead to physically unrealistic results that are unsatisfactory.

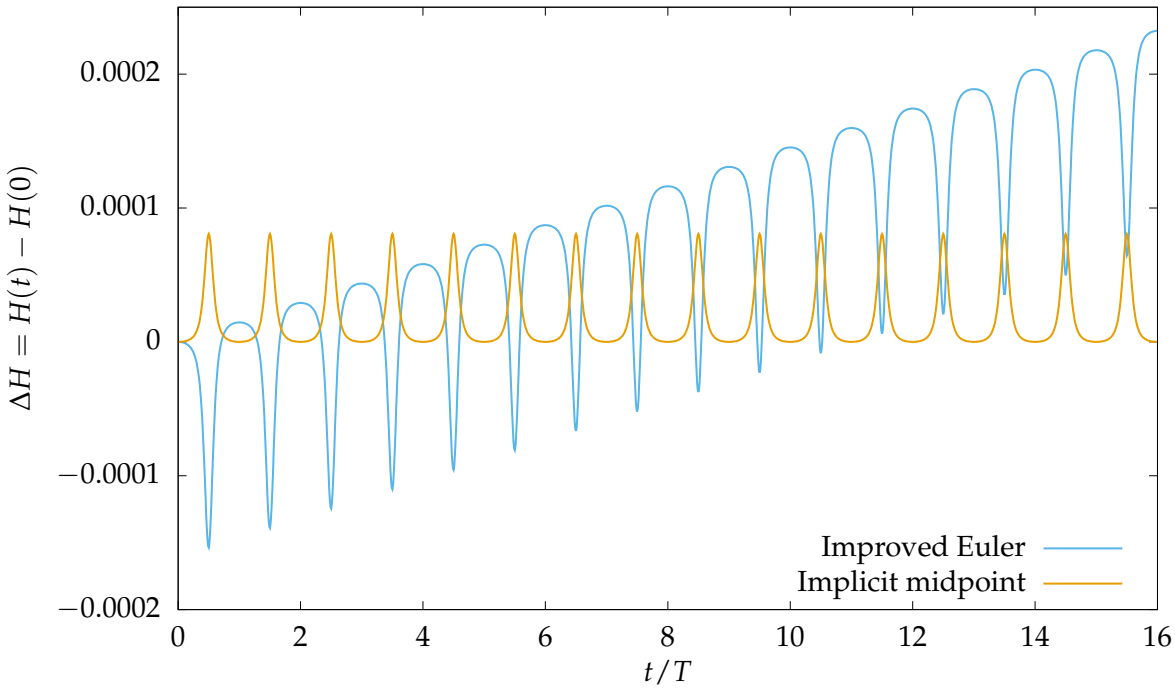

Figure 2: Changes in time in the Hamiltonian for the improved Euler method and implicit midpoint method, applied to the elliptical orbit test problem. The horizontal axis is scaled in terms of orbital periods $T = 2\pi$.

The other two methods are much better at capturing the elliptical orbit shape, and are near-indistinguishable from the true result. To examine these methods in detail, Fig. 2 shows the change in the Hamiltonian over a long integration duration of $16T = 32\pi$. Over many periods, the improved Euler method exhibits a small upward drift in the Hamiltonian, meaning that eventually the asteroid spirals outward, similar to the forward Euler method. The implicit midpoint method behaves differently: while there are some small variations in H, there is no observable drift even after many periods. As we shall see, the implicit midpoint method is symplectic.

Some symplectic methods

We now switch to using subscripts on p and q to denote the timestep. A one-step numerical method with step size h is generally given by mapping $\psi_h : \mathbb{R}^{2n} \to \mathbb{R}^{2n}$ that takes a given step from (p_0, q_0) to (p_1, q_1). For implicit methods, it is possible that the mapping may not exist for certain values of (p_0, q_0), in which case we may have to restrict the domain of the mapping.

Definition 1 *A one-step method is called symplectic if for every smooth Hamiltonian and every step size h the mapping ψ_h is symplectic, so that it preserves the differential 2-form in Eq. 3.*

It can be shown that the implicit midpoint method is indeed a symplectic method. Given a Hamiltonian, the flow induced by Eq. 1 is symplectic. It is worth noting that Definition 1 states that a numerical method is symplectic if the mappings ψ_h for any Hamiltonian are symplectic, but this does not guarantee that ψ_h will preserve the Hamiltonian from which it is derived. Hence the behavior of ΔH for the implicit midpoint method shown in Fig. 2 is typical, where symplecticity ensures that there is no overall drift, but small variations in ΔH are visible over one orbital period.

In lecture 5, we observed that implicit midpoint method can be derived by considering one-point Gaussian quadrature over a step of size h. Furthermore, Kuntzmann and Butcher showed that every s-point Gaussian quadrature scheme has a corresponding s-stage implicit Runge–Kutta scheme of order $2s$. It turns out that all of these methods are symplectic, as given by the following theorem—see Hairer *et al.* [1] for full details of the proof.

Theorem 1 *The implicit s-stage Kuntzmann & Butcher methods of order $2s$ are symplectic for all values of s.*

For a general s-stage implicit Runge–Kutta scheme with coefficients a_{ij} and b_j, the following theorem provides constraints that must be satisfied in order for the method to be symplectic. Again, the proof of this theorem is quite long and the reader should consult Hairer *et al.* [1] for complete details.

Theorem 2 *If the $s \times s$ matrix M with elements*

$$m_{ij} = b_i a_{ij} + b_j a_{ji} - b_i b_j \tag{14}$$

satisfies $M = 0$, then the Runge–Kutta method is symplectic.

One consequence of Theorem 2 is that explicit Runge–Kutta methods can never be symplectic. To see this, consider the ith diagonal term of M. Since $a_{ii} = 0$ for an explicit method, it follows that

$$m_{ii} = b_i a_{ii} + b_i a_{ii} - b_i b_i = b_i \times 0 + b_i \times 0 - b_i^2 = -b_i^2, \tag{15}$$

and hence $b_i = 0$ for all i. This is not a valid method since it implies that $(p_1, q_1) = (p_0, q_0)$ and thus no update takes place.

Partitioned Runge–Kutta methods

Since Hamiltonian systems depend on two sets of variables, the p and the q, it is natural to consider partitioned methods that integrate the two parts differently. Consider

$$P_i = p_0 + h \sum_j a_{ij} k_j, \qquad Q_i = q_0 + h \sum_j \hat{a}_{ij} l_j, \tag{16}$$

$$p_1 = p_1 + h \sum_j b_i k_i, \qquad q_1 = q_0 + h \sum_i \hat{b}_i l_i, \tag{17}$$

$$k_i = -\frac{\partial H}{\partial q}(P_i, Q_i), \qquad l_i = \frac{\partial H}{\partial p}(P_i, Q_i) \tag{18}$$

where $a_{ij}, \hat{a}_{ij}, b_i, \hat{b}_i$ are the coefficients for two different s-stage Runge–Kutta schemes. For this situation, there is a generalization of Theorem 2 as follows [1].

Theorem 3 *If the coefficients satisfy*

$$b_i = \hat{b}_i \tag{19}$$

for $i = 1, \ldots, s$ *and*

$$b_i \hat{a}_{ij} + \hat{b}_j a_{ji} - b_i \hat{b}_j = 0 \tag{20}$$

for $i, j = 1, \ldots, s$ *then the method is symplectic. Furthermore, if the Hamiltonian is separable, so that* $H(p, q) = T(p) + U(q)$*, then Eq. 20 is sufficient for the method to be symplectic.*

The additional freedom allows new methods to be derived. In particular, for the separable Hamiltonian case, we could search for a method that is diagonally implicit in p and explicit in q, such that

$$a_{ij} = 0 \quad \text{for } i < j, \qquad \hat{a}_{ij} = 0 \quad \text{for } i \leq j. \tag{21}$$

Furthermore, since the Hamiltonian is separable, $\partial H/\partial q = \partial U/\partial q$ and therefore the update formula for p becomes explicit. The condition from Eq. 20 places strong restrictions on the coefficients in the method. One finds that

$$a_{ij} = b_j \quad \text{for } i \geq j, \qquad \hat{a}_{ij} = \hat{b}_j \quad \text{for } i > j. \tag{22}$$

Hence we obtain the Butcher tableaus

$$\begin{array}{lllll} b_1 & & & & \\ b_1 & b_2 & & & \\ b_1 & b_2 & b_3 & & \\ \vdots & \vdots & \ddots & \ddots & \\ b_1 & b_2 & \cdots & b_{s-1} & b_s \\ \hline b_1 & b_2 & \cdots & b_{s-1} & b_s \end{array} \qquad \begin{array}{lllll} 0 & & & & \\ \hat{b}_1 & 0 & & & \\ \hat{b}_1 & \hat{b}_2 & 0 & & \\ \vdots & \vdots & \ddots & \ddots & \\ \hat{b}_1 & \hat{b}_2 & \cdots & \hat{b}_{s-1} & 0 \\ \hline \hat{b}_1 & \hat{b}_2 & \cdots & \hat{b}_{s-1} & \hat{b}_s \end{array}$$

for p and q respectively. Since methods of this form at defined by two sets of terms, the more compact notation

$$\begin{array}{lllll} b: & b_1 & b_2 & \ldots & b_s \\ \hat{b}: & \hat{b}_1 & \hat{b}_2 & \ldots & \hat{b}_s \end{array} \tag{23}$$

is introduced. Methods of this form are particularly straightforward to implement, as shown in the following algorithm:

$P_0 = p_0, Q_1 = q_0$
for $i \in \{1, 2, \ldots, s\}$ **do**
  $P_i = P_{i-1} - h b_i \partial U/\partial q(Q_i)$
  $Q_{i+1} = Q_i + h \hat{b}_i \partial T/\partial p(P_i)$
end
$p_1 = P_s, q_1 = Q_{s+1}$

Note that P_i depends only on P_{i-1} and Q_i, while Q_{i+1} depends only on Q_i and P_i. Hence p and q can be updated in place, without the need to allocate extra memory for additional steps, as is usually required for multi-step Runge–Kutta method.

A simple example of method of this form is the one-step method

$$\begin{array}{ll} b: & 1 \\ \hat{b}: & 1, \end{array} \tag{24}$$

which combines an backward Euler step for p with a forward Euler step for q, resulting in an order 1 method as follows:

$$p_1 = p_0 - h\frac{\partial U}{\partial q}(q_0), \qquad q_1 = q_0 + h\frac{\partial T}{\partial p}(p_1). \tag{25}$$

Note that the roles of p and q can be reversed, which leads to the alternative method

$$q_1 = q_0 + h\frac{\partial T}{\partial p}(p_0), \qquad p_1 = p_0 - h\frac{\partial T}{\partial q}(q_1). \tag{26}$$

This can be written as

$$\begin{array}{lll} b: & 0 & 1 \\ \hat{b}: & 1 & 0 \end{array} \tag{27}$$

in the notation introduced above. The method given by Eq. 27 is called the *adjoint* of the method in Eq. 24. By considering the order conditions, one can derive higher-order methods, such as the following third-order method due to Ruth:

$$\begin{array}{lccc} b: & 7/24 & 3/4 & -1/24 \\ \hat{b}: & 2/3 & -2/3 & 1. \end{array} \tag{28}$$

Using the adjoint to derive higher order methods

The adjoint of a general method given by Eq. 23 is

$$\begin{array}{lccccc} b: & 0 & b_s & b_{s-1} & \dots & b_2 & b_1 \\ \hat{b}: & \hat{b}_s & \hat{b}_{s-1} & \hat{b}_{s-2} & \dots & b_1 & 0, \end{array} \tag{29}$$

which can be derived by switching the roles of (p_0, q_0) & (p_1, q_1), and taking a timestep of length $-h$. One way to derive a new method is to concatenate a step of size $h/2$ of Eq. 23 with a step of size $h/2$ of its adjoint, yielding

$$\begin{array}{lccccccccc} b: & b_1/2 & b_2/2 & \dots & b_{s-1}/2 & b_s/2 & b_s/2 & b_{s-1}/2 & \dots & b_2/2 & b_1/2 \\ \hat{b}: & \hat{b}_1/2 & \hat{b}_2/2 & \dots & \hat{b}_{s-1}/2 & \hat{b}_s & \hat{b}_{s-1}/2 & \hat{b}_{s-2}/2 & \dots & \hat{b}_1/2 & 0. \end{array} \tag{30}$$

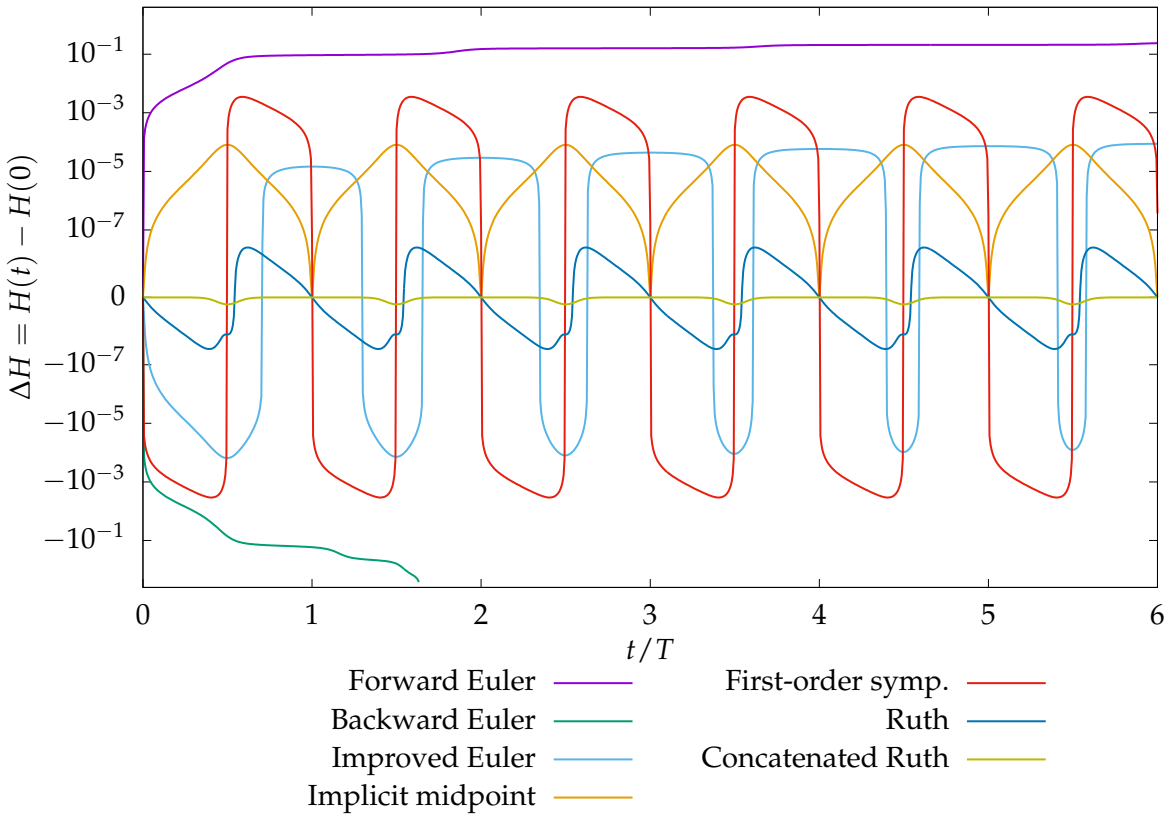

Figure 3: Changes in the Hamiltonian for the asteroid problem for seven different methods. A nonlinear mapping $f(x) = \sinh^{-1}(10^9 x)$ is applied to the vertical axis in order to show the wide range of scales. The horizontal axis is scaled in terms of orbital periods $T = 2\pi$.

Due to the concatenation, the two half steps of size $\hat{b}_s/2$ are combined into one step of size $\hat{b}_s$. Because of symmetry, Eq. 30 must have even order. Hence, if this procedure is applied to a method of odd order, it results in an increase in the order of the method. Applying the approach to Ruth's method in Eq. 28 yields the fourth-order method

$$\begin{array}{lcccccc} b: & 7/48 & 3/8 & -1/48 & -1/48 & 3/8 & 7/48 \\ \hat{b}: & 1/3 & -1/3 & 1 & -1/3 & 1/3 & 0. \end{array} \tag{31}$$

Accuracy tests for the symplectic methods

Figure 3 shows a plot of the change in Hamiltonian for the orbit test problem. The plot shows the original four methods, plus the three methods for separable Hamiltonian introduced above: the first-order method (Eq. 24), Ruth's third-order method (Eq. 28), and the fourth-order concatenated improvement (Eq. 31). A nonlinear mapping is applied to the vertical axis in order to show the wide variety of scales.

To test accuracy, the asteroid orbit problem is simulated over a duration of two complete periods, $2T = 4\pi$. The exact solution is therefore the same as the initial condition. Figure 4(a) shows a work–precision plot for the seven methods. The first-order forward Euler and backward Euler methods are inefficient, and the backward Euler method requires at least 20000 function evaluations to avoid an invalid solution in the fixed-point root finding routine. The two implicit methods are not as efficient as a corresponding explicit method of the same order. However, in these test codes, the tolerance on the fixed point iteration is set to be very stringent, only terminating when the change in solution is below $10^{-12.5}$ for five consecutive iterations.

For the separable Hamiltonian methods, each calculation of $\partial H/\partial p$ and $\partial H/\partial q$ is counted as half of a function evaluation. The first-order symplectic method exhibits second-order accuracy for this case, due to a cancellation of the leading-order error term. Similarly, Ruth's third-order method actually exhibits fourth-order accuracy for this case. Since the fourth-order concatenated method involves taking two steps of the third-order method, the efficiency of the two is near-identical. However, the fourth-order method is slightly more efficient, since each step only requires ten half-evaluations. Since $\hat{b}_6 = 0$ is zero, this saves one half-evaluation. Furthermore, the steps for b_1 and b_6 both use the same evaluation of $\partial h/\partial q$ and thus this only needs to be evaluated once.

To break the symmetry associated with completing an integer number of periods, Fig. 4(b) shows a work–precision plot for a duration of 15. The plot is similar to Fig. 4(a), although the first-order symplectic method loses its additional accuracy. Interestingly, the third-order Ruth method still exhibits fourth-order accuracy. It is likely that the specific form of the Hamiltonian for the orbit problem leads to the cancellation of leading-order error terms.

References

[1] E. Hairer, S. P. Nørsett, and G. Wanner, *Solving Ordinary Differential Equations I: Nonstiff Problems*. Springer, 1993.

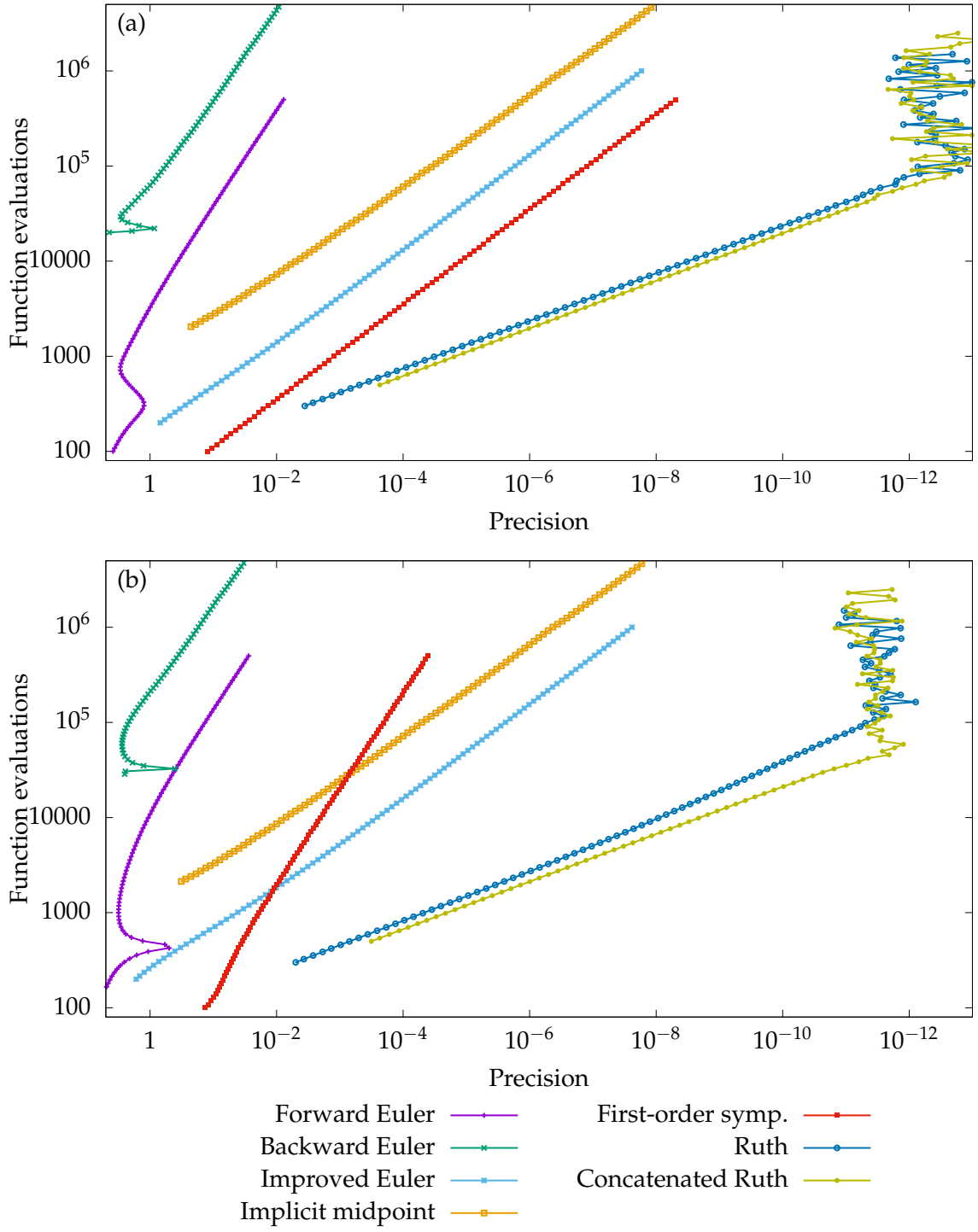

Figure 4: Work–precision plots for the seven different methods applied to the asteroid test problem. The precision is based on the Euclidean norm between the true solution and the computed solution, calculated at (a) $t = 4T$ corresponding to two complete orbits, and (b) $t = 15$ corresponding to a non-complete orbit.